ERT imaging of a shallow basin: eastern Lago Fagnano, Tierra del Fuego, Argentina

A. Tassone[1], M.G. Santomauro[1], M. Menichetti[2], M.E. Cerredo[3], E. Lodolo[4], M.B. Remesal[3], H. Lippai[1], J.L. Hormaechea[5] and J.F. Vilas[1]

[1] *CONICET-Instituto de Geofísica Daniel A. Valencio (INGEODAV), Buenos Aires, Argentina*
[2] *Istituto di Scienze della Terra, Urbino, Italy*
[3] *CONICET-Departamento de Geología, Buenos Aires, Argentina*
[4] *Istituto Nazionale di Oceanografia e di Geofisica Sperimentale (OGS), Trieste, Italy*
[5] *Estación Astronómica Río Grande (EARG), Argentina*

(Received: March 22, 2010; accepted: September 16, 2010)

ABSTRACT Two ERT (Electrical Resistivity Tomography) profiles were conducted at the eastern head of Lago Fagnano within the main deformation zone of the Magallanes-Fagnano Transform fault system (MFS) which represents the onland boundary between the South America and Scotia plates. Results from the inversion models have provided new evidence of the presence and location, at shallow depths, of some strands of the MFS. Tomographic models showed significant resistivity contrasts across the inferred fault zones in the subsurface. The combination of ERT, geomorphic and outcrop structural data allowed us to interpret the stepped, southward subsidence of Tertiary and Quaternary units within the studied area. The Holocene development and evolution of a shallow deltaic basin at the mouth of Río Turbio, the eastern tributary of Lago Fagnano, was also interpreted from electrical imaging.

1. Introduction

The westernmost segment of the South America-Scotia plate boundary traverses the central region of Tierra del Fuego. It is defined by the Magallanes-Fagnano Fault System (MFS), which is a sinistral transtensional tectonic lineament (Lodolo *et al*., 2002). Several asymmetric and restricted pull-apart basins, many tens of kilometres long and a few kilometres wide occur within the principal deformation zone of the MFS, both in the Atlantic and in the Pacific offshore as well as in the onshore areas (Polonia *et al*., 1999; Bartole *et al*., 2000; Lodolo *et al*., 2003; Menichetti *et al*., 2004; Tassone *et al*., 2005, 2008). The main on land strike-slip related basin is represented by the Lago Fagnano, located in the northern flank of the Fuegian Andes (Fig. 1a) and infilling a mostly asymmetric depression 105 km long, 7 km wide, and ca. 200 m deep, below sea level (Lodolo *et al*., 2003, 2007; Waldmann *et al*., 2008).

A bathymetric survey has showed that the Lago Fagnano is the surface expression of at least two large pull-apart basins (Fig. 2), formed by strands of the MFS (Lodolo *et al*., 2003, 2007). The transverse Rio Claro fault separates the highly asymmetric basin of the eastern Lago Fagnano from the central, symmetrical part of the lake. The eastern sub-basin is highly asymmetric with flat depocentral areas and reaches the most significant depths (210 m). The main depocentre is located near the main MFS fault, along the northern coast of the lake. The steeper slope of the basin, along the northern shore of the Lago Fagnano coincides with the most pronounced regional topographic

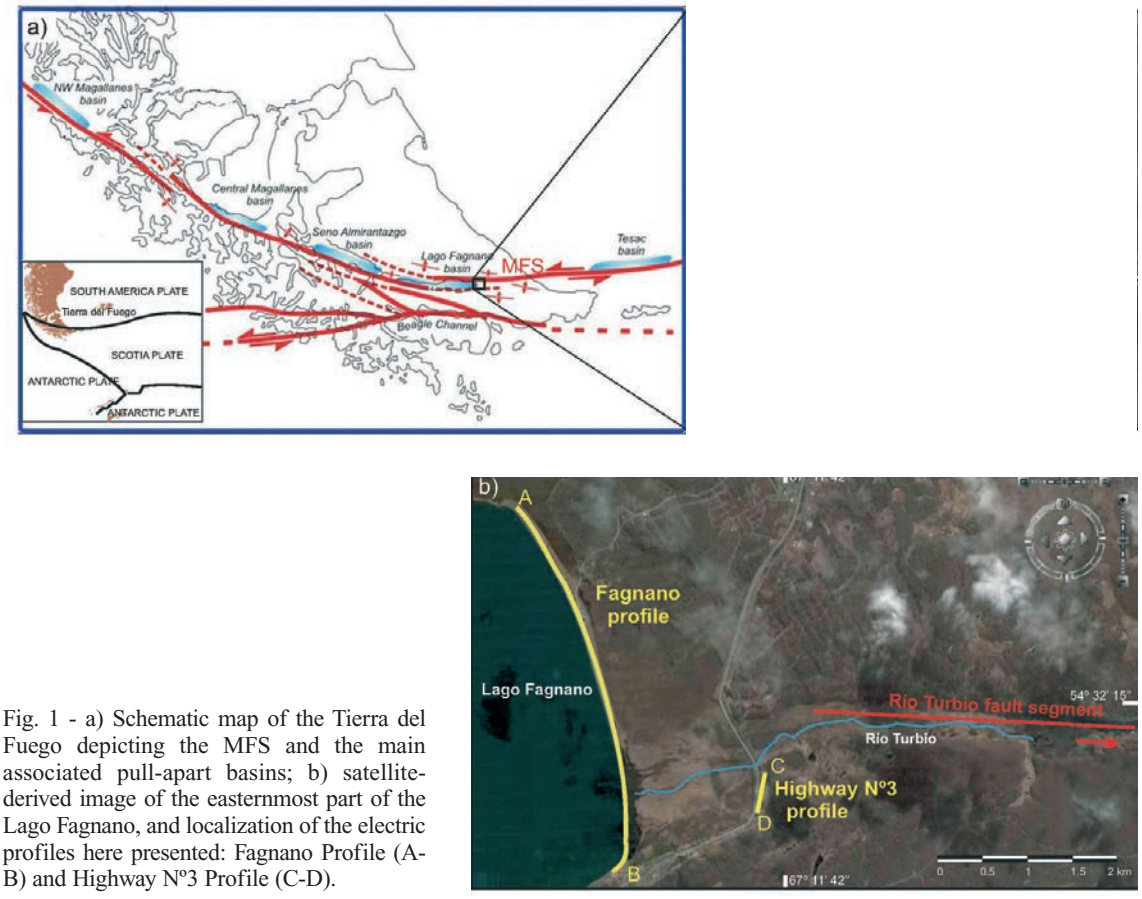

Fig. 1 - a) Schematic map of the Tierra del Fuego depicting the MFS and the main associated pull-apart basins; b) satellite-derived image of the easternmost part of the Lago Fagnano, and localization of the electric profiles here presented: Fagnano Profile (A-B) and Highway N°3 Profile (C-D).

gradient which was possibly generated by the action of the fault strand in this sector of the Lago Fagnano (Lippai *et al*., 2003; Lodolo *et al*., 2007). Seismic sections have confirmed the asymmetrical geometry of the basin characterized by a steep northern margin (Waldmann *et al*., 2008, 2010).

Inmmediatly to the east of Lago Fagnano, a broadly E-W, 18–20 km long, trending segment corresponds to a narrow (about 300 m wide), steep-sided and linear depression occupied by the Rio Turbio Valley, the eastern tributary of Lago Fagnano, which represents a master segment of the MFS (Fig. 1b). This lineament (Fig. 3) is associated with relative gravity minima at both ends and a less pronounced minimum along the valley occupied by the Rio Turbio (Lodolo *et al*., 2003, 2007). The presence of the local relative gravity minima and their associated mass deficiencies, correspond to the locus of distinct basins formed within the principal displacement zone of the MFS.

By means of two geoelectrical transects, we have investigated the sag pond located just to the east of the eastern shore of the Lago Fagnano in correspondence to the surface expression of a sedimentary basin developed between the Rio Turbio segment and the eastern Lago Fagnano basin. The results obtained have been combined with field geologic information and satellite images, with the purpose of defining the continuity of the fault segments that compose the MFS in the area.

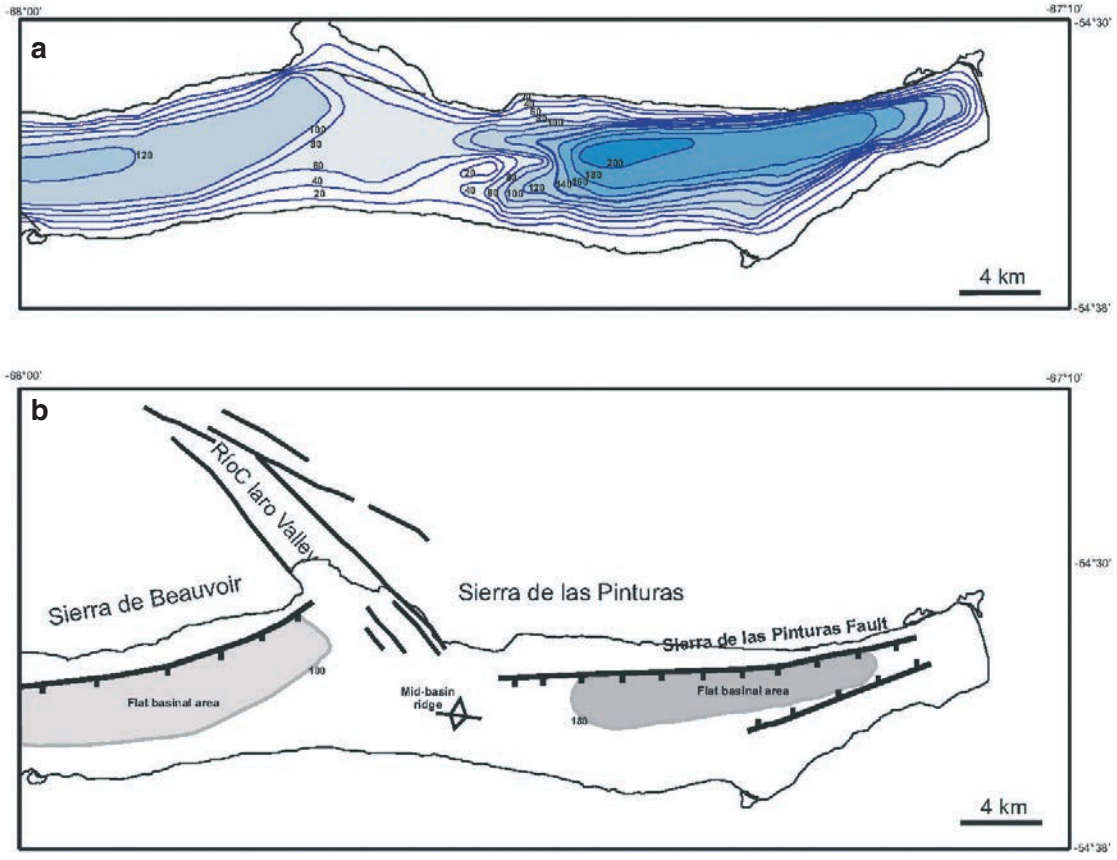

Fig. 2 - a) Central eastern Lago Fagnano simplified bathymetric map: b) simplified structural interpretation. The central eastern Lago Fagnano is composed of at least two pull-apart basins characterized by flat depocentral areas, and separated by an important splay fault (the Rio Claro transverse fault). A morphological high separates the two depocenters (after Lodolo *et al.*, 2007).

The electrical resistivity tomography method (ERT) is a quick, non-invasive and low-cost geophysical method widely applied to obtain 2-D, high-resolution imaging of the resistivity subsurface pattern. ERT has shown to be a useful method to determine the location of faults, to analyze their kynematics and to study the structural setting of geological sedimentary basins (Fleta *et al*., 2000; Giano *et al*., 2000; Storz *et al*., 2000; Suzuki *et al*., 2000; Verbeek *et al*., 2000; Demanet *et al*., 2001a, 2001b; Caputo *et al*., 2003, 2007; Wise *et al*., 2003; Colella *et al*., 2004; Rizzo *et al*., 2004; Nguyen *et al*., 2005, 2007).

2. Geological framework

The eastern Fagnano basin was formed by a main E-W striking, subvertical master fault, the Río Turbio-Las Pinturas fault segments that represent the bounding structures of the principal deformation zone of the MFS (Figs. 2 and 4) in this area. The Sierra de las Pinturas fault segment, running roughly parallel along the northern shore of the lake, forms a releasing step-over and

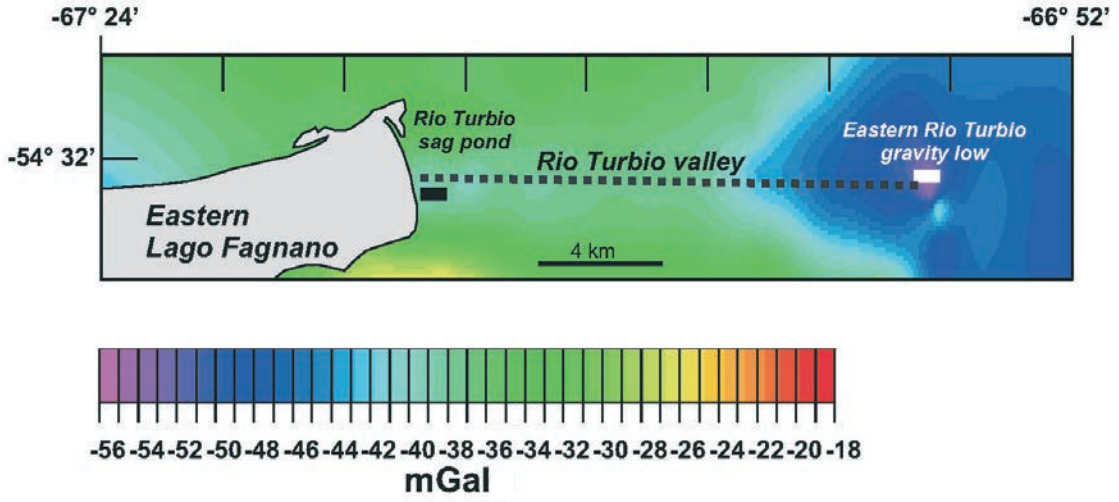

Fig. 3 - Bouguer gravity map of the eastern part of the Lago Fagnano area and Rio Turbio Valley (from Lodolo *et al.*, 2007). The two distinct relative gravity minima (represented by a minus sign) are indicated: one located just to the east of the Lago Fagnano eastern shore (a sag pond); the other at the eastern termination of the Rio Turbio Valley. Both anomalies run along the trace of the Rio Turbio valley.

developed secondary, splay transversal extensional structures responsible for the pull-apart basin development. The Río Turbio and Sierra de las Pinturas fault segments are subvertical and E-W striking for at least 30 km, characterized by sub-horizontal striae on subvertical surfaces indicating strike-slip dominant displacement; kinematic indicators consistently show sinistral strike-slip displacement (Menichetti *et al*., 2008).

The morphology of the eastern Lago Fagnano is dominated by the glacial processes that developed after the Last Glacial Maximum. The deposits are represented by a frontal moraine complex surrounding the lake head (the Tolhuin-Jeu Jepen moraine complex) which includes ground and lateral moraine structures, kame deposits in the margins and a glaciolacustrine plain in the front. The frontal complex is interrupted by the Río Turbio depression (Fig. 4) where a delta develops (Coronato *et al*., 2002, 2005, 2009). The restricted outcrops of the Fuegian fold-and-thrust belt, represented by the sedimentary rocks of the Paleogene Río Claro Formation (Camacho, 1967), have been also glacially overridden (Coronato *et al*., 2009).

Aligned fault scarps, truncated vegetation, and sag ponds are expressions of the MFS activity within the studied area. South of Tolhuin, the Río Turbio fault cuts across the glacial fluvio-lacustrine Quaternary sediments displaying several eroded scarps, thus providing evidence for a recent dip-slip fault reactivation (Lodolo *et al*., 2003). The glaciolacustrine sediments are deformed by several sets of WNW–ESE, sub-vertical, south-dipping normal faults with a prevalent left-lateral transtensional component. The fluvial drainages are clearly controlled by the presence of the E–W structures related to the strike-slip faults with several capture corners, as in the upper part of the valley that hosts the Turbio River (Menichetti *et al*., 2004). The neotectonic activity of the fault system is also put in evidence by a W-E scarp of about 1 m, corresponding to a stepped gravel barrier on the Lago Fagnano shore that originated a sag pond of the lower Río

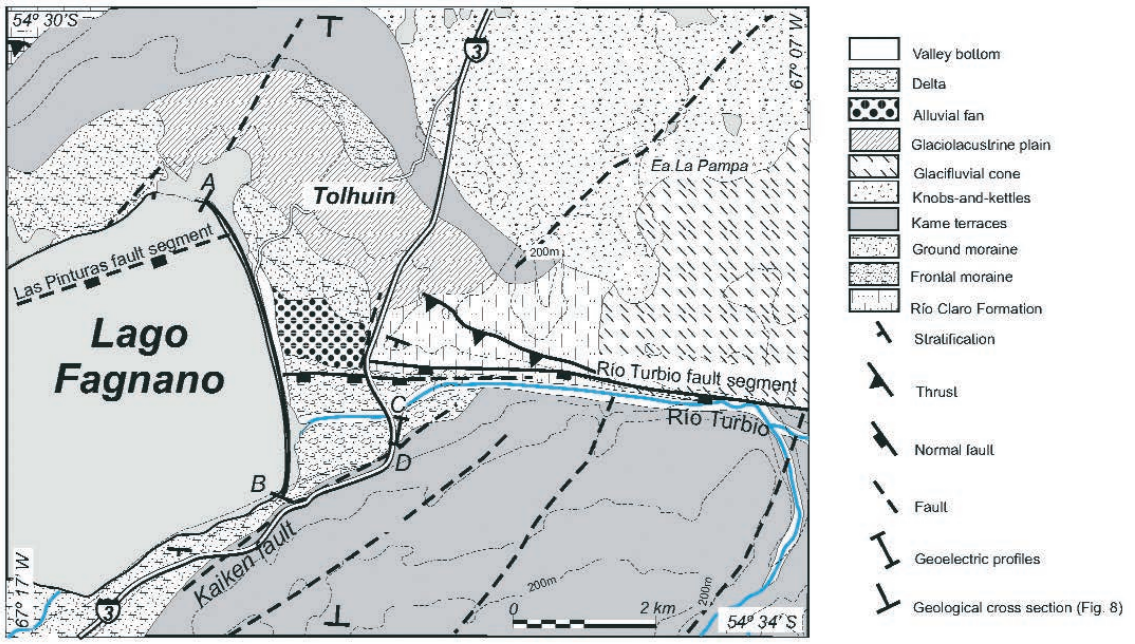

Fig. 4 - Detailed geologic map east of Lago Fagnano combining geomorphic cartography (after Coronato *et al.*, 2002) with own field surveys and image interpretation of fault structures. Location of the ERT Fagnano profile (A – B) and the Highway Nº3 profile (C – D).

Turbio valley (Lodolo *et al*., 2002).

3. Field acquisition and data inversion

3.1. Field data acquisition

The field survey consisted of two geo-electric transects acquired: (1) along the eastern shore of Lago Fagnano, and (2) along its eastern region, beside Highway Nº3 (Fig. 4). The resistivity profile which runs parallel to the eastern shore of Lago Fagnano, has a broad N-S orientation and is almost 4 km long (Fagnano Profile); the Highway Nº3 Profile is about 2.5 km from the Fagnano Profile, presents a NNE-SSW direction and is 0.4 km long.

Resistivity measurements were performed with a Syscal R1 resistivity-meter system. The electrodes are connected on the back of the resistivity-meter by means of two strings of heavy-duty seismic-like cable with 24 out-put each, conforming a linear array of 48 electrode nodes, with a 10 m of maximum spacing. A further extension to 72 or more electrodes can be done by applying the roll along technique.

Acquisition and geometric parameters (maximum permitted standard deviation of the measurement, minimum and maximum numbers of stacks per measurement, input current time per cycle and desired signal voltage) have to be set. The resistivity-meter is able to automatically perform the pre-defined sets of measurements according to the type of array selected and provides direct reading of the input current, potential difference, electrode location and apparent resistivity. Geometric parameters level and electrode spacing were assigned according to the

desired maximum depth of investigation and noise level.

The resistivity method was applied with a Wenner-Schlumberger array that provides a high vertical resolution and a high signal-to-noise ratio (Dahlin and Zhou, 2004). In spite of its lower horizontal resolution in relation to other arrays, the Wenner-Schlumberger array is sensitive to both horizontal and vertical resistivity variations. The selected array provides not only a better horizontal coverage but also the maximum depth of penetration is 15% larger than the Wenner array (Loke, 1997).

The chosen spacing between electrodes was: 10 m for levels 1-5, 20 m for levels 6-8, and 40 m from level 9. The Fagnano Profile required the roll-along method to cover the whole of the measurement profile of almost 4 km. Once the sequence of measurements was completed, the cable was moved a few spacing units on the electric profile. This way, measurements made from connected electrodes were repeated, while new measurements (taken from new electrodes) defined a parallelogram-shaped pseudo-section. With this technique, two measurement sequences of 470 m were performed, each one followed by 12 roll-along sequences, adding 120 m of profiling each time. The investigation depths depend on the number of levels chosen, the electrode separation, the total length of profiles and the type of array. In our case, the investigation depths reached around 70 m.

3.2. Data inversion

In order to get a resistivity tomography, the obtained resistivity pseudo-sections were processed with an inversion software to obtain 2-D models of the study area.

Two dimensional resistivity tomographies provide a resistivity distribution section of a subsurface portion of the Earth from potential measurements made at the surface. The measured pseudo-section (Figs. 5a1 and 5b1) is a contour diagram where the apparent resistivity values are assigned to a predefined location according to the array type used (Telford *et al*., 1990). As depths of investigation are pseudo-depths and resistivities are apparent, the pseudo-section offers a qualitative scenario of the subsurface resistivity distribution.

Inversion methods attempt to find a model (an idealized mathematical representation) of the resistivity distribution of a sub-surface section from tension measurements made on the surface. The 2-D model used by the inversion program (RES2DINV) of the Geotomo software (Loke, 1996-2002, 2001). Consists of a number of rectangular blocks. The arrangement of the blocks is loosely tied to the distribution of the data points in the pseudo-section and each one of these has its own value of resistivity. The depth of the bottom row of blocks is set to be approximately equal to the equivalent depth of investigation of the data points with the largest electrode spacing. From apparent resistivity measurements (field pseudo-section, Figs. 5a1 and 5b1) the software offers an initial model that predicts a series of calculated, apparent resistivity values (model pseudo-section, Figs. 5a2 and 5b2). These values are compared with those obtained from the measurements. The comparison of such values modifies the model as many times as the difference between them is below a cutoff. A measure of this difference is given by the root-mean-squared (RMS) error (Figs. 5a3-4 and 5b3). The inversion process is based on the comparison of pseudo-sections because they include both resistivities and geometry. We applied the smoothness-constrained least-squares method (deGroot-Hedlin and Constable, 1990) that makes resistivity spatial variations become smooth by minimizing the square difference between

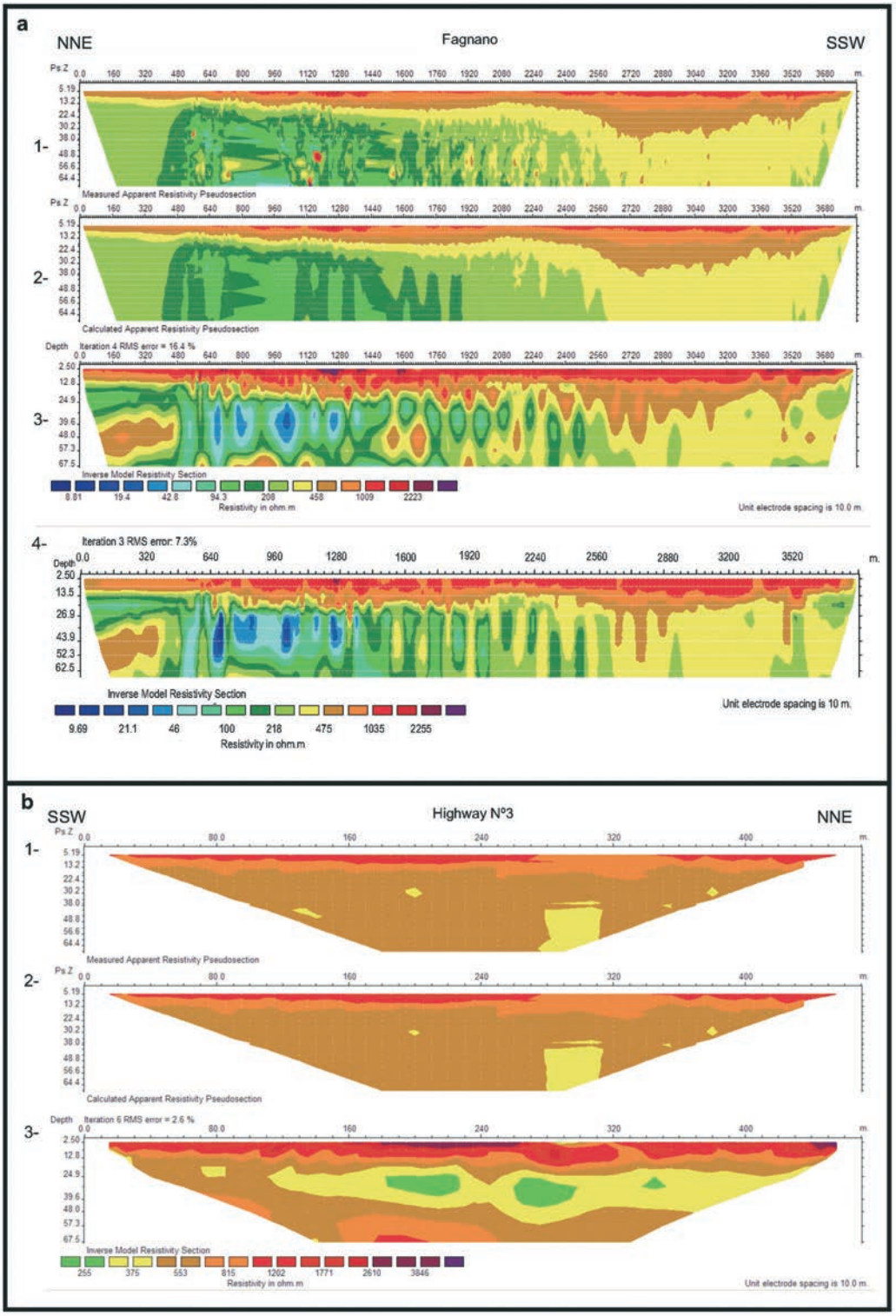

Fig. 5 - Resistivity distribution along Fagnano profile (a) and Highway Nº 3 profile (b): 1 - measured apparent resistivity pseudo-section, 2 - calculated apparent resistivity pseudo-section, 3 and 4 - inverse model resistivity section. Location of resistivity profiles on Fig. 4.

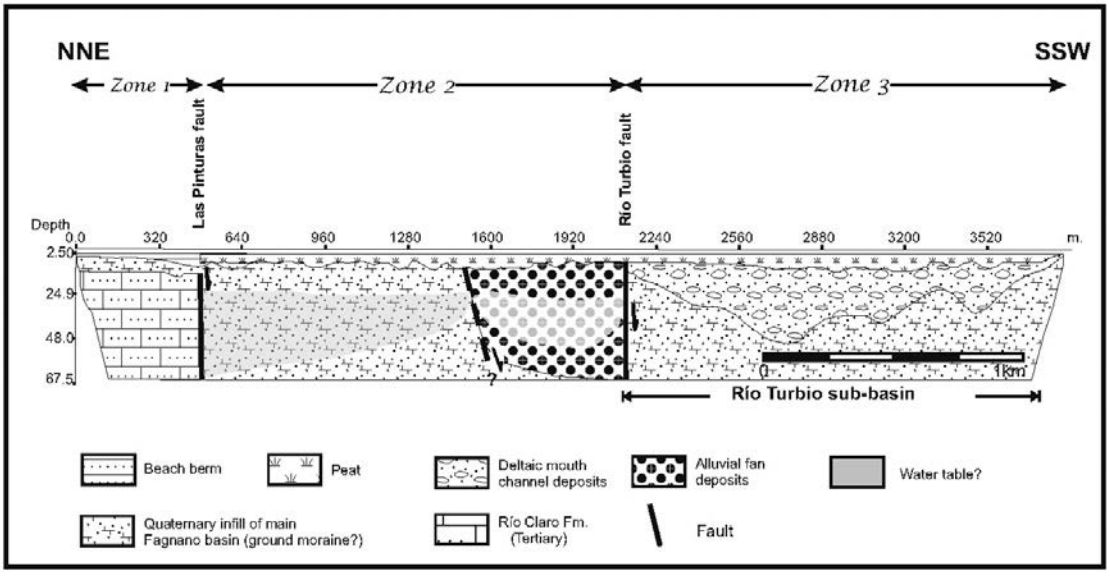

Fig. 6 - ERT section of the Fagnano profile. Location in Fig. 5: a) inverse model resistivity section, b) geologic section interpreted from the resistivity model.

apparent resistivity measurements and calculated apparent resistivity values.

Fig. 5 shows the inversion models obtained for the Fagnano (Fig. 5a3) and Highway Nº3 (Fig. 5b3) profiles. The low RMS error (<3) of the latter indicates that the model is accurate; therefore a reliable interpretation may be drawn from this ERT profile. Given the high RMS (16.4%) of the Fagnano profile (Fig. 5a3) yielded by the smoothness-constrained least squares (L_2-norm) inversion method, we performed a robust inversion (L_1-norm) for this tomography (Fig. 5a4). Although somewhat "blocky", the inversion model obtained after 3 iterations yielded a significantly lower RMS (7.3%). The overall pattern of resistivity distribution obtained with both inversion methods shows a remarkable similarity, indicating that the results are geophysically robust.

4. Results

Fig. 6 shows the geological interpretation derived from the ERT analysis of the Fagnano profile. The electric tomography (Figs. 5a3 and 5a4), with a modeled maximum penetration depth of ~ 67 m, displays an upper resistive layer (around 5 m-thick) which correlates well with the shore gravels and the widespread peat deposits. The high resistivity of the peat is attributed to the low ph and ionic concentration of the peat pore water. The underlying levels show significant variations of resistivity values both vertically and horizontally, indicating that subsurface materials are strongly differentiated by their electric properties. On the basis of the lateral distribution of resistivity values, three zones were distinguished in the ERT section and interpreted in the geological section (Fig. 6).

Zone 1. A strong resistivity contrast at about 480 m from the beginning of the profile separates

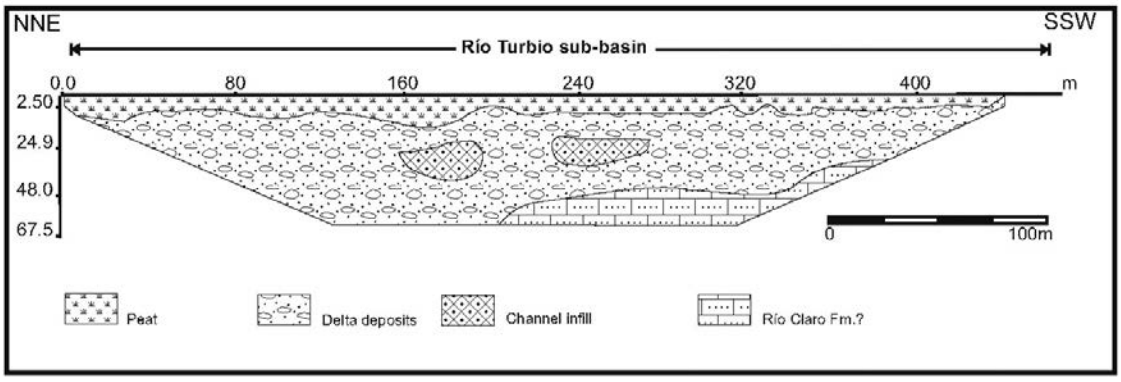

Fig. 7 - ERT section of the Highway Nº3 profile: a) inverse model resistivity section, b) geologic section interpreted from the resistivity model.

a region with low resistivities (20-40 Ωm) to the south, from a region with higher resistivities (>300 Ωm) to the north. This feature stands around the eastern projection of the Las Pinturas fault segment (Fig. 4). Therefore, the sharp lateral variation in resistivities is interpreted as related to the presence of a main sub-vertical, blind fault, buried under the moraine deposits with no geomorphic expression. The interpreted fault separates low-resistivity sediments to the south, from high-resistivity materials to the north, possibly pertaining to the Paleogene sedimentary rocks Río Claro Fm that outcrop in the area (Fig. 4).

Zone 2. In the central sector of the tomography (from ~ 480 to ~2000 m) very low resistivity values (< 40 Ωm) occur at intermediate levels (~ 25-50 m). Within this zone, two well defined bodies with fairly regular tops at around 20 m depth can be distinguished, the southern one displays a wedge-shaped morphology and has the lowest resistivities ($\rho < 20$ Ωm), whereas the northern one shows overall concave-up outline and slightly higher resistivity values. We interpret them as indicating the presence of significant ground water content (water table?).

The southern boundary of this zone is defined by the projection of the subvertical Río Turbio fault. The segment of the ERT profile comprised between the interpreted continuities of the Las Pinturas and Río Turbio faults enclose water tables likely hosted in the buried moraine and alluvial fan deposits cropping out some hundred meters eastwards of the profile. Therefore, the interpreted watertables would be bounded by the Las Pinturas and Río Turbio faults which behave as barriers channelizing water circulation coming from the east.

A steep, south-dipping fault is speculatively inferred between the two interpreted water tables, on the basis of the important lateral changes in resistivity values in the deepest part of the model.

Zone 3. The southern portion (from ~2000 m to the end of the profile), in turn, shows a shallow body with a fairly flat top and concave base with intermediate resistivity (~500-1000 Ωm) from 10 to 50 m depth underlying the peat bog deposits. On the surface, this zone corresponds to the deltaic accumulations of Rio Turbio.

The extensional movements along the RTF could have resulted in the development of this small basin (the Río Turbio sub-basin, Fig. 6) which is also recognizable on the satellite image (Fig. 1). The general asymmetry of the basin with a likely northward shift in depocenters suggests

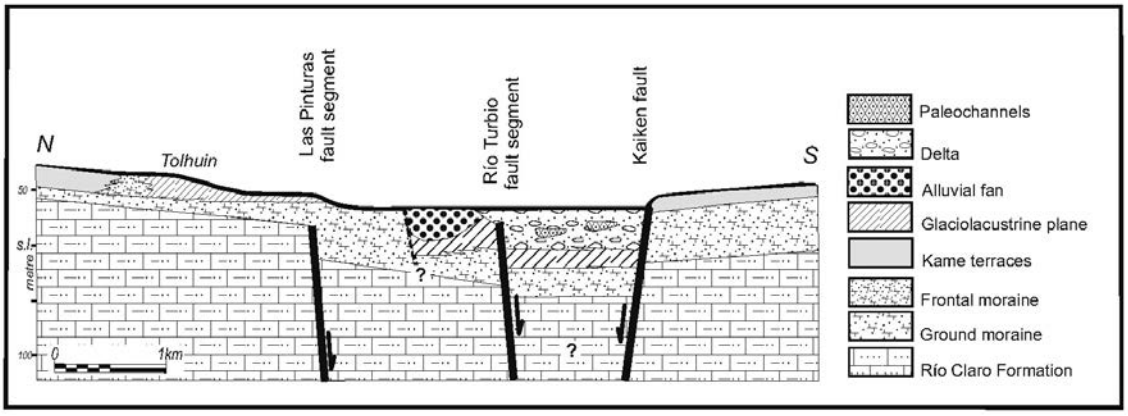

Fig. 8 - Schematic cross-section of the easternmost Fagnano basin, built by combining ERT and geological outcrop data. Location in Fig. 4.

that the fault may have controlled the displacement of the Río Turbio, from a southern position to a northern one. The neotectonic activity of this fault is also put in evidence on Quaternary deposits affected by E-W trending, south-dipping, sub-vertical faults (Menichetti *et al*., 2004).

The Highway Nº3 inverse model (Fig. 5b) shows a cross profile of the southern portion of the Rio Turbio sub-basin with several significant vertical variations of resistivity values with depth, possibly due to the increment of water content in sediments up to 40 m depth. Localized high resistivity values up to 1000 Ωm are found in the lowermost part of the ERT section (around 65 m depth). The probable presence of buried Paleogene sedimentary rocks underlying the Quaternary deposits can not be ruled out. Two low resistivity, rounded areas are noticeably between 25 and 45 m depth which might correspond to the Río Turbio palaeo-channels. The river migration within the basin may have been strongly controlled by the differential movements along the Kaiken fault (Fig. 4) a splay of the Río Turbio fault.

5. Discussion

A schematic N-S cross-section (Fig. 8) was built by combining field information with ERT interpretations; this profile cuts across the Río Turbio sub-basin at average altitudes similar to those of the Fagnano profile and some 10 m lower than the CD ERT. Fig. 8 shows the shallow architecture of the eastern Fagnano area bounded by the eastern projection of Las Pinturas fault segment to the north, whereas a NE-SW splay of the Rio Turbio fault segment (Kaiken fault) marks its southern boundary.

The motions along the interpreted faults have thrown down blocks of the Paleogene Río Claro Formatione yielding a compartmented basin filled with glaciolacustrine and glacifluvial facies. The ground moraines of the Tolhuin-Jeu Jepen complex of the early recessional phase (~ 21000 yr BP), of Fagnano palaeoglacier (Coronato *et al*., 2009) advanced over a substratum mainly made of the sedimentary rocks of the Río Claro Formation fossilizing the eastern continuity of Las Pinturas fault segment in the northern area. By this time, an outwash plane formed eastwards

(partly represented by the glacifluvial cone and the knobs-and-kettles landforms of Fig. 4) drained by the palaeo-Turbio river which flowed NE-wards to the Atlantic coast (Coronato *et al*., 2002).

The early dissection of the frontal Tolhuin-Jeu Jepen complex was likely the result of a combined isostatic rebound after glacial recession and tectonic movements. The uplift of the previously glacially overridden hills of the Río Claro Formation along a splay of Las Pinturas Fault triggered the accumulation of the alluvial fan (Figs. 4 and 8).

Extensional movements along the Río Turbio fault provoked a dramatic change in the drainage network and further dissection of the Tolhuin moraine as it forced the Río Turbio to flow westwards into the Fagnano basin, as indicated by capture corners (Menichetti *et al*., 2004). The Río Turbio sub-basin evolved between the Río Turbio fault and its splay, the Kaiken fault. The Early Holocene age of Río Turbio basal peat bog (Coronato *et al*., 2009) provides an upper constraint for the deltaic sub-basin. The significant northward thickening of basin infill points to a younger activity along the southern Kaiken fault.

Our ERT surveys combined with structural information points to a southward trend in the fossilization of the different fault segments that represent the main deformation zone of the MFS in the area.

The present morphology of the eastern areas of Fagnano are the result of glacial advancing and retreating pulses, later overprinted by alluvial and fluvial accumulations, strongly controlled by tectonic activity along distinct fault segments of the MFS.

6. Conclusions

Two electrical resistivity tomographies were acquired at the eastern termination of Lago Fagnano. The ERT sections provided useful information that allowed the characterization of the link between the two main fault segments of the MFS in the easternmost Fagnano basin, i.e., the Sierra de las Pinturas and the Rio Turbio. The subsurface orientation of the fault planes obtained from ERT images combined with structural surface data allowed us to recognize the trend in fault activity and the development of a shallow basin, the Río Turbio sub-basin.

The electrical images obtained are consistent with previous structural information supporting near-vertical to high-angle fault planes mostly of extensional nature.

The ERT method was a valuable tool to recognize fault planes at subsurface which were identified either as a zone with a significantly lower resistivity or as narrow zones with a remarkably high resistivity contrast. The lateral variation of electrical resistivity on both sides of these structures allowed us to infer areas where the fault plane acted as a hydrogeological barrier.

Our ERT survey combined with outcrop features highlights the significant role of the transverse fractures in shaping and delimiting the shallow basins and deposits. This role has been already noticed for the transverse Río Claro fault which separates the main Fagnano basin into eastern and western basins (Lodolo *et al*., 2003)

Acknowledgements. The authors acknowledge the critical comments of the reviewers that significantly improved the final version. This study was supported by grants from CONICET, Agencia Nacional Científica y Tecnológica and University of Buenos Airea (Argentina). The Estación Astronómica Rio

Grande (EARG) greatly contributed during the field operations. The authors are particularly indebted to Gerardo O´Connon, Carlos Ferrer, and Luis Barbero (of the EARG) for their support with geodesic data acquisition.

REFERENCES

Bartole R., Colizza E., De Muro S. and Colautti W.; 2000: *The Pacific entrance of the Magellan Strait: preliminary results of a seismic and sampling survey.* Terra Antarctica Reports, **4**, 81-94.

Camacho H.; 1967: *Las transgresiones del Cretácico superior y Terciario de la Argentina*. Revista de la Asociación Geológica Argentina, **22**, 253-260.

Caputo R., Piscitelli S., Oliveto A., Rizzo E. and Lapenna V.; 2003: *The use of electrical resistivity tomographies in active tectonics: examples from Tyrnavos Basin, Greece.* J. Geodynamics, **36**, 19-35.

Caputo R., Salviulo L., Piscitelli S. and Loperte A.; 2007: *Late Quaternary activity along the Scorciabuoi Fault (Southern Italy) as inferred from electrical resistivity tomographies.* Annals of Geophysics, **50**, 213-223.

Colella A., Lapenna V. and Rizzo E.; 2004: *High-resolution imaging of the High Agri Valley Basin (Southern Italy) with electrical resistivity tomography.* Tectonophysics, **386**, 29-40.

Coronato A., Roig C. and Mir X.; 2002: *Geoformas glaciarias de la región oriental del Lago Fagnano, Tierra del Fuego, Argentina.* In: Cabaleri N., Cingolani C., Linares E., López de Luchi M., Ostera H. and Panarello H. (eds), XV Congreso Geológico Argentino, pp. 457–462.

Coronato A., Seppälä M. and Rabassa J.; 2005: *Last Glaciation landforms in Lake Fagnano ice lobe, Tierra del Fuego, southernmost Argentina.* In: 6th International Conference on Geomorphology, Zaragoza, Spain.

Coronato A., Seppälä M., Ponce F. and Rabassa J.; 2009: *Glacial geomorphology of the Pleistocene Lake Fagnano ice lobe, Tierra del Fuego, southern South America: Alpine and lowland glacial landscape*. Geomorphology, **112**, 67–81.

Dahlin T. and Zhou B.; 2004: *A numerical comparison of 2D resistivity imaging with 10 electrode arrays.* Geophysical Prospecting, **52**, 379-398.

deGroot-Hedlin C. and Constable S.; 1990: *Occam´s inversion to generate smooth, two dimensional models for magnetotelluric data.* Geophysics, **55**, 1613-1624.

Demanet D., Pirard E., Renardy F. and Jongmans D.; 2001a: *Application and processing of geophysical images for mapping faults.* Computers and Geosciencies, **27**, 1031-1037.

Demanet D., Renardy F., Vanneste K., Jongmas D., Camelbeeck T. and Meghraoui M.; 2001b: *The use of geophysical prospecting for imaging active faults in the Roer Graben, Belgium*. Geophysics, **66**, 78-89.

Fleta J., Santanach P., Martinez P., Goula X., Grellet B. and Masana E.; 2000: *Geologic, geomorphologic and geophysic approaches for the paleoseismological analysis of the Amer fault (NE Spain).* In: Workshop Proceedings of HAN2000, Evaluation of the potential for large earthquakes in regions of present day low seismic activity in Europe, Han-sur-Lesse, Belgium, pp. 63–66.

Giano S.I., Lapenna V., Piscitelli S. and Schiattarella M.; 2000: *Electrical imaging and self-potencial surveys to study the geological setting of the Quaternary slope deposits in the Agri high valley (Southern Italy)*. Annali di Geofisica, **43**, 409-419.

Lippai H., Lodolo E., Tassone A., Hormaechea J.L., Menichetti M. and Vilas J.F.; 2003: *Morphostructure of Lago Fagnano (Tierra del Fuego) and adjacent areas.* Boll. Geof. Teor. Appl., 45, Supp. 2, 142-144

Lodolo E., Lippai H., Tassone A., Zanolla C., Menichetti M. and Hormaechea J.L.; 2007: *Gravity map of the Isla Grande de Tierra del Fuego and morphology of Lago Fagnano.* Geologica Acta, **5**, 307-314.

Lodolo E., Menichetti M., Tassone A., Bartole R. and Ben-Avraham Z.; 2003: *Magallanes-Fagnano continental transform fault (Tierra del Fuego, southernmost South America).* Tectonics, **22**, 1076, doi:10.1029/2003TC001500.

Lodolo E., Menichetti M., Tassone A., Geletti R., Sterzai P., Lippai H. and Hormaechea J.L.; 2002*: Researchers target a continental transform Fault in Tierra del Fuego.* EOS Transactions AGU, **83**, 1-6.

Loke M.H.; 1996-2002: *Tutorial: 2-D and 3-D electrical imaging surveys.* Geotomo Software, 136 pp.

Loke M.H.; 1997: *Electrical imaging surveys for environmental and engineering studies – a practical guide to 2D and 3D surveys.* Geotomo Software, 68 pp.

Loke M.H.; 2001: *Rapid 2-D resistivity and IP inversion using the least-squares method. Geoelectrical Imaging 2-D and 3-D.* Geotomo Software, 81 pp.

Menichetti M., Lodolo E. and Tassone A.; 2008: *Structural geology of the Fuegian Andes and Magallanes fold-and-thrust belt – Tierra del Fuego Island.* Geologica Acta, **6**, 55-67.

Menichetti M., Acevedo R.D., Bujalesky G.G., Cenni M., Cerredo M.E., Coronato A., Hormachea J.L., Lippai H., Lodolo E., Olivero E.B., Rabassa J. and Tassone A.; 2004: *Geology and geophysics of Isla Grande de Tierra del Fuego.* In: Field-trip guide, Geosur 2004, Argentina, pp. 39.

Nguyen F., Garambois S., Chardon D., Hermitte D., Bellier O. and Jongmans D.; 2007: *Subsurface electrical imaging of anisotropic formations affected by a slow active reverse fault, Provence, France.* J. App. Geophys., **62**, 338-353.

Nguyen F., Garambois S., Jongmans D., Pirard E. and Loke M.H.; 2005: *Image processing of 2D resistivity data for imaging faults.* J. App. Geophys., **57**, 260-277.

Polonia A., Brancolini G., Torelli L. and Vera E.; 1999: *Structural variability at the active continental margin off Southernmost Chile.* J. Geodynamics, **27**, 289-307.

Rizzo E., Colella A., Lapenna V. and Piscitelli S.; 2004: *High-resolution images of the fault-controlled High Agri Valley basin (Southern Italy) with deep and shallow electrical resistivity tomographies.* Physics and Chemistry of the Earth, **29**, 321-327.

Storz H., Storz W. and Jacobs F.; 2000: *Electrical resistivity tomography to investigate geological structures of the Earth's upper crust.* Geophysical Prospecting, **48**, 455-471.

Suzuki K., Toda S., Kusunoki K., Fujimitsu Y., Mogi T. and Jomori A.; 2000: *Case studies of electrical and electromagnetic methods applied to mapping active faults beneath the thick quaternary*. Engineering Geology, **56**, 29-45.

Tassone A., Lippai H., Lodolo E., Menichetti M., Comba A., Hormaechea J.L. and Vilas J.F.; 2005: *A geological and geophysical crustal section across the Magallanes-Fagnano fault in Tierra del Fuego and associated asymmetric basins formation.* J. South America Earth Sc., **19**, 99-109.

Tassone A., Lodolo E., Menichetti M., Yagupsky D., Caffau M. and Vilas J.F.; 2008: *Seismostratigraphic and structural setting of the Malvinas Basin and its southern margin (Tierra del Fuego Atlantic offshore)*. Geologica Acta, **6**, 19-42.

Telford W.M., Geldart L.P. and Sheriff R.E.; 1990: *Applied Geophysics.* Cambridge University Press, Cambridge, 790 pp.

Verbeeck K., Beatse H., Vanneste K., Renardy F., Van Der Meer H., Roy-Chowdhury K. and Camelbeeck T.; 2000: *Geomorphic and geophysical reconnaissance of the Reppel and Bocholt faults, NE Belgium.* In: Workshop proceedings of HAN2000, Evaluation of the potential for large earthquakes in regions of present day low seismic activity in Europe, Han-sur-Lesse, Belgium, pp. 167-170.

Waldmann N., Ariztegui D., Anselmetti F.S., Austin Jr. J.A., Coronato A. and Austin J.A.; 2008: *Seismic stratigraphy of Lago Fagnano sediments (Tierra del Fuego, Argentina) - A potential archive of paleoclimatic change and tectonic activity since the Late Glacial.* Geologica Acta, **6**, 101-110.

Waldmann N., Ariztegui D., Anselmetti F.S., Austin Jr. J.A., Dunbar R., Moy C.M. and Recasens C.; 2010: *Geophysical evidence of multiple glacier advances in Lago Fagnano (54ºS), southernmost Patagonia.* Quaternary Sc. Rev., **29**, 1188-1200.

Wise D.J., Cassidy J. and Locke C.A.; 2003: *Geophysical imaging of the Quaternary Wairoa North Fault, New Zealand: a case study*. J. App. Geophys., **53**, 1-16.

Corresponding author: Alejandro Tassone
Istituto de Geofísica, Dep. Ciencias Geológical Universidad
Pabellón 2, Buenos Aires, Argentina
Phone: +54 11 47883439; fax: +54 11 47883439; e-mail: atassone@ge.fcen.uba.ar